Research Article

Chemical Review and Letters
journal homepage: www.chemrevlett.com
ISSN (online): 2645-4947 (print) 2676-7279

Synthesis characterization and gas sensing properties of Ni and Fe modified nanocrystalline SnO_2 thick film sensors

Vinayak Bagul[1], Ganesh Bhagure[2], Bhushan Langi[2], Deepak Tayde[3*]

[1] *Department of Chemistry, Arts, Science, and Commerce College, Surgana-422211 India*
[2] *Department of Chemistry, Satish Pradhan Dyansadhana College of Arts, Science and Commerce, Thane-400601, India*
[3] *Department of Chemistry, Mahant Jamnadas Maharaj Arts, Commerce and Science college, Karanjali-422208, India*
**e-mail:dtt_chem@yahoo.com; phone: +919421983158 and fax No: 02558-234666*

ARTICLE INFO

Article history:
Received 08 March 2024
Received in revised form 8 May 2024
Accepted 13 June 2024
Available online 24 June 2024

Keywords:
Co-precipitation method
Metal Doping
SnO_2-nanomaterial
Sensing Properties

ABSTRACT

Ni and Fe doped SnO_2 Nanocrystalline material were synthesized by co-precipitation method. We study the structural, morphological properties by XRD and SEM-EDS analysis of newly doped Ni doped SnO_2 and Fe doped SnO_2 material. After getting good results for this material, we study the gas sensing properties such as the stability, selectivity, response and recoverability after that which is utilized as gas sensor for the investigation of some toxic and volatile gases those are dangerous to the environment.

1. Introduction

According to recent data from the United Nation Environment Program (UNEP) there are 7 million premature deaths every year due to air pollution. The air pollution and climate change problems are closely related to each other and create the greatest environmental hazard to public health worldwide [1]. There are CO_2, CO, H_2S, NO_2, SO_2, Lead, Ammonia, Methane, Gasoline and various VOC (Volatile Organic Compounds) pollutants in the environment produced by urbanization and deforestation of nature, Those points have directly effect on the surface of water and soil to contaminate there purity hence they are very toxic and dangerous to living life on earth [2][3].

19^{th} century Dr. Oliver Johanson invented the first modern catalytic gas sensor, which was introduced to the world for safety purposes [4]. After that, Silicon Valley first electronic company was established to prepare the first combined instrument which was a detector of both combustible gases and oxygen. The metal oxide semiconductor (MOS) was investigated in 1990 and after that, it will be reserve its place in the field of gas sensors and have a very important rank in the environmental gas detector era.[5].

The gas detectors were classified as electrochemical, catalytic beads, photoionization, infrared points, infrared imaging and semiconductors [6]. Nowadays, semiconducting materials consisting of metal oxides are wildly used as sensing materials in domestic, commercial and industrial fields [7-9].

The toxic and VOC containing gases, such as NO_2 gas, it is easily absorbed in the lungs of living thing, due to its chemical and physical properties and cause heart failure due to inhalation [10]. If the concentration of NH_3 in the blood increases, then it may be to associate with coma or convulsions [11]. Ethanol is a volatile organic compound, taking a high dose of it causes Hypothermia, Hypoglycaemia, and is extensor rigidity and also attributed to the development of malnutrition. Continued or everyday contact may result in a liver injury [12] [13]. Central nervous system and respiratory depression happened due to the toxicity of H_2S gas, and most important information is that there is no verified antidote for this poisoning [14] [15]. Detecting such deadly toxic gases and saving lives

∗ Corresponding author.; e-mail: dtt_chem@yahoo.com
https://doi.org/10.22034/crl.2024.447531.1307

thing by utilizing the metal doped SnO_2 material is really interesting to us.

Recently, lots of metal doped semiconducting materials were used as gas sensors, such as at room temperature, the rutile structure with a tetragonal structure is the most common and extensively used SnO_2 sensor [16]. Sn_4 occupies the top and center of the tetrahedron in the SnO_2 cell of the tetragonal rutile structure, while O_2 occupies specified positions within the structure. Each SnO_2 crystal cell is composed of 2 Sn and 4 O elements [17]. Many scientists in recent years have worked to improve the gas-sensing capabilities of SnO_2 materials by preparing them with novel materials. One-dimensional (1D) SnO_2 nanostructures, such as wires, rods, tubes, and belts, are promising for sensitive gas sensors due to their distinctive shape, structure, and surface area [18-22].

Introducing dopants is a typical method for improving gas sensor performance. Noble metal dopants, including Au, Ag, Pt, and Pd enhance gas sensing properties in SnO_2, [23] but their expensive cost limits their practical usage. Consider using less expensive materials such as common transition metals (e.g., Fe, Co, Ni, and Cu) to improve sensing performance and minimize costs.

The SnO_2 gas sensing mechanism is based on the change in resistance that is generated by a change in the concentration of electrons that is caused by the adsorption or desorption of gas: The SnO_2 material exhibits the ability to adsorb oxygen from the surrounding air and subsequently break it down into oxygen ions [24]. This process leads to a modification of the potential barrier between the grains of SnO_2, thereby inducing a variation in the resistance (conductivity) of the gas sensor. When the sensor comes into contact with the gas to be detected, the molecules of the gas react with the oxygen anions that have been adsorbed by the sensor [25]. As a result of the oxygen electrons that had been trapped being released back into the conduction band of SnO_2, the resistance of the SnO_2 gas sensor has decreased [26][27]. However, the sensing performances of traditional SnO_2-based gas sensors still have several drawbacks, including high working temperatures and low selectivity. These problems can be caused by a number of factors. The classic form of SnO_2 has less active sites, which limits the adherence of oxygen atoms to its surface. As a result, the sensing performance of this form of SnO_2 is inadequate [28]. Therefore, in this article, we will go through the preparation methods for manufacturing nanostructured SnO_2, as well as the detection of different types of gases and element doping. In this research work, we will discuss the work done by our group as well as the work done by other groups in the field of SnO_2 sensors, as well as the current research development and the potential for SnO_2 gas sensors in the future. The well-known n-type wide band gap semiconductor (Eg = 3.6 eV) rutile-structured SnO_2 has attracted considerable attention due to its various potential applications [29].

In this work, we report the effective synthesis of Ni and Fe doped well aligned layered SnO_2 nanoarrays by a co-precipitation technique. Although the undoped SnO_2 nanostructure is effective as a gas sensor, it is limited by some restrictions, such as a high working temperature and low sensitivity.

2. Experimental

Synthesis of Ni and Fe doped SnO_2 Nanomaterials

Transition metal doped SnO_2 nanoparticle were prepared by co-precipitation method [30]. To be prepared separately $SnCl_4$ $5H_2O$ (1g) and Ni (NO_3) H_2O (1g) were dissolved in deionized distilled water with constant stirring at room temperature for 30 min to get the clear solution. Then add Ni (NO_3) H_2O solution dropwise in the colloidal solution of $SnCl_4$ $5H_2O$ solution with constant stirring for 1h. After the proper mixing of these two solutions, add 5 mL of NH_4OH to maintain the $P^H = 9$ to 10 of the solution to make the solution basic, and the precipitate is obtained. Then the mixture was stir for 1 h to get the homogeneous precipitate. The precipitate mixture were filtered with simple filter paper, and after 3-4 times washing with distilled water, the precipitate was obtained. This precipitate was then dried in precipitate in oven for 2 h at 85^{o}C. The dried sample were crushed in mortal and piston to prepare the fine powder and calcined at 500^{o}C for 2 h in a muffle furnace under air. After the natural cooling, the powder were again grind in mortal and piston to get the Ni-doped SnO_2 nanomaterial. Follow the same procedure for the preparation of Fe-doped SnO_2 nanoparticles.

Fabrication of Ni and Fe doped SnO_2

Screen printing is a cost effective technique where the mesh is used to prepare the thick film of the material on the substrate. Here we used the constant ratio 30:70 of organic to inorganic materials. Here, the organic material act as a binder which is made up of butyl carbitol acetate (BCA) and Ethyl cellulose (EC) those were used to fix the particle doped nanomaterial to the glass surface. To prepare the fine nanoparticles of Nickel doped SnO_2. To take the 0.7g of Ni doped SnO_2 in the mortar with the addition of a pinch of Ethyl cellulose (EC), grind for 30 min with the help of a piston. To make a smooth paste, add BCA dropwise in the mixture. Then take the cut piece of glass measuring 3cm by 1.5 cm, on which the pseudo plastic paste was spread over 20 thick layers of the same material. After that dry this film for 45 mins in Infra-red lamp and then heat it for 2 hr

at 500 ^{0}C in a muffle furnace. After the natural cooling the next day, thick film sensor materials were used for exciting gas sensing research. To repeat the same procedure for the preparation of thick film by using Fe dopant SnO_2.

3. Results and discussion

Powder X-ray Diffraction

The structural arrangements of Ni and Fe doped SnO_2 were studied using PXRD at the angle of 2θ between 10° to 80°. Figure 1 illustrate the XRD pattern of Ni and Fe doped SnO_2. The Ni doped SnO_2 clearly indicate the main characteristic peaks (110), (101), (200) and (211) appeared at 2θ angels 26.57°, 33.88°, 37.93° and 51.76° respectively. The observed diffraction peak were noticed as tetragonal structure [31]. The Fe doped SnO_2 report the 2θ value 26.68°, 33.95°, 38.06°, 51.85°, 54.88°, 64.78° which indicate the miller indices (110), (101), (020), (121), (220) and (112) planes respectively. The plane (020) and (121) indicate the doping of Fe metal is successful. From the calculating the diffraction peak were observed orthorhombic structural geometry [32]. Apparent crystalline size were obtained by Scherrer equation [33] formula $D = K\lambda / \beta \cos \theta$ where K is the scherrer constant, λ is the wavelength of the x-ray beam, Full width at half maximum (FWHM) of the peak has represents β and θ is Bragg angel. Table 1 shows the crystalline size of Ni doped SnO_2 is 16.33 nm and Fe doped SnO_2 have 14.06 nm.

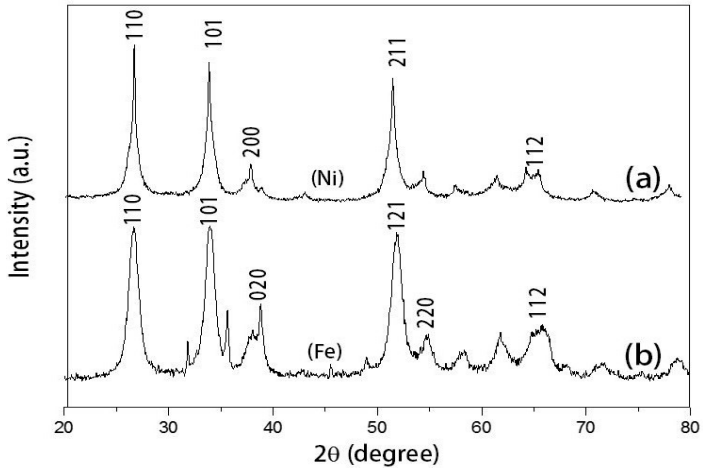

Fig. 1. XRD pattern of (a) Ni doped SnO_2 and (b) Fe doped SnO_2.

Table 1. Average crystallite sizes of material was determined by using Scherrer equation.

Entry	Sample	Average crystallite size (nm)
1	Ni doped SnO_2	16.33
2	Fe doped SnO_2	14.06

SEM and EDS Analysis

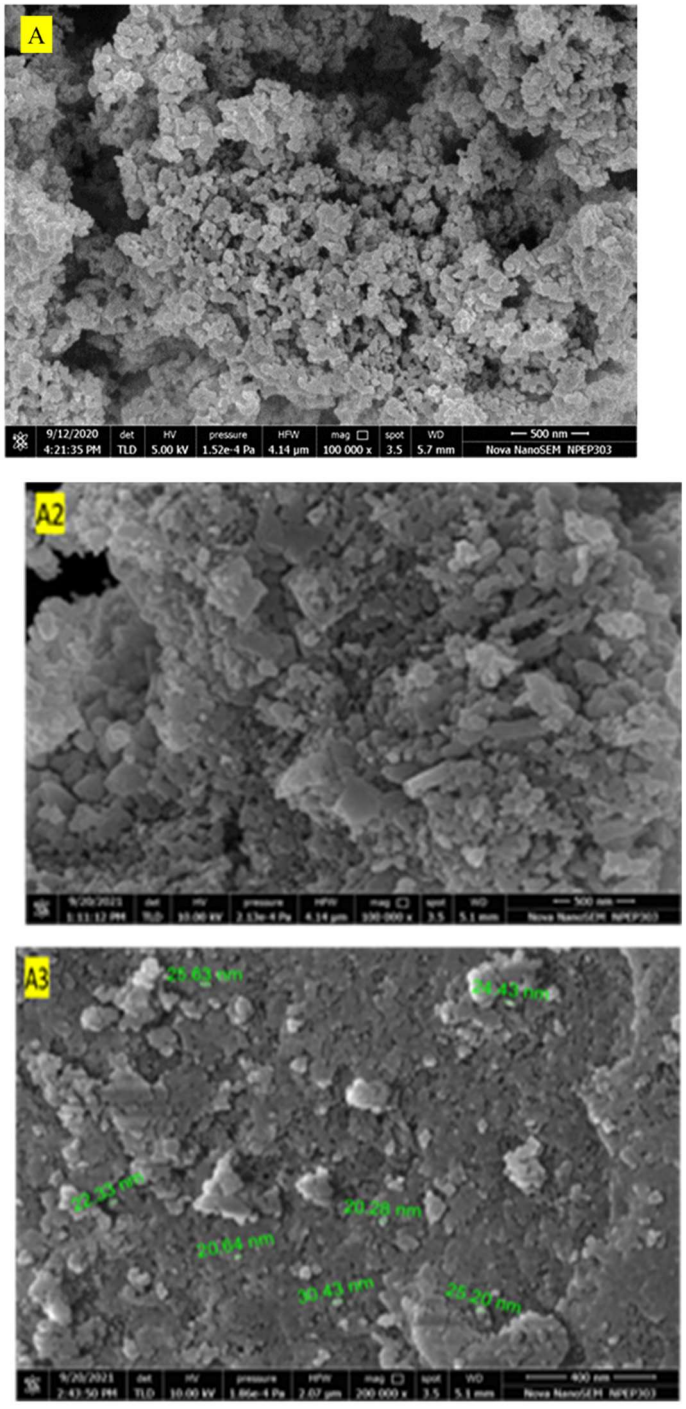

Fig. 2. SEM images of (A) Undoped SnO_2, (A2) Ni doped SnO_2 and (A3) Fe doped SnO_2.

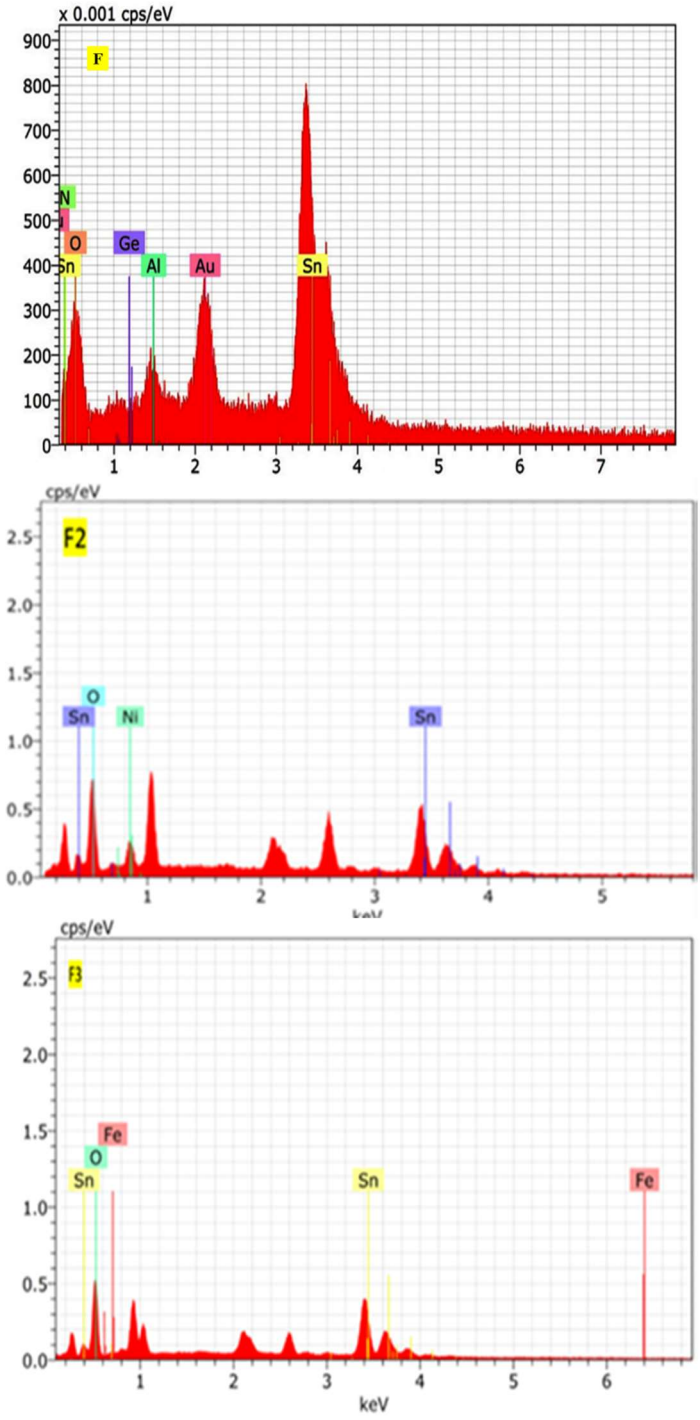

Fig. 3. EDS spectra of (F) Undoped SnO_2, (F2) Ni doped SnO_2 and (F3) Fe doped SnO_2.

Scanning Electron Microscopy was employed to investigate the shape, size and surface morphology of the material with the help of scattered electron from the particle surface. In the figure 2 (A) show the undoped SnO_2 have small grains with agglomeration of particles on the surface.

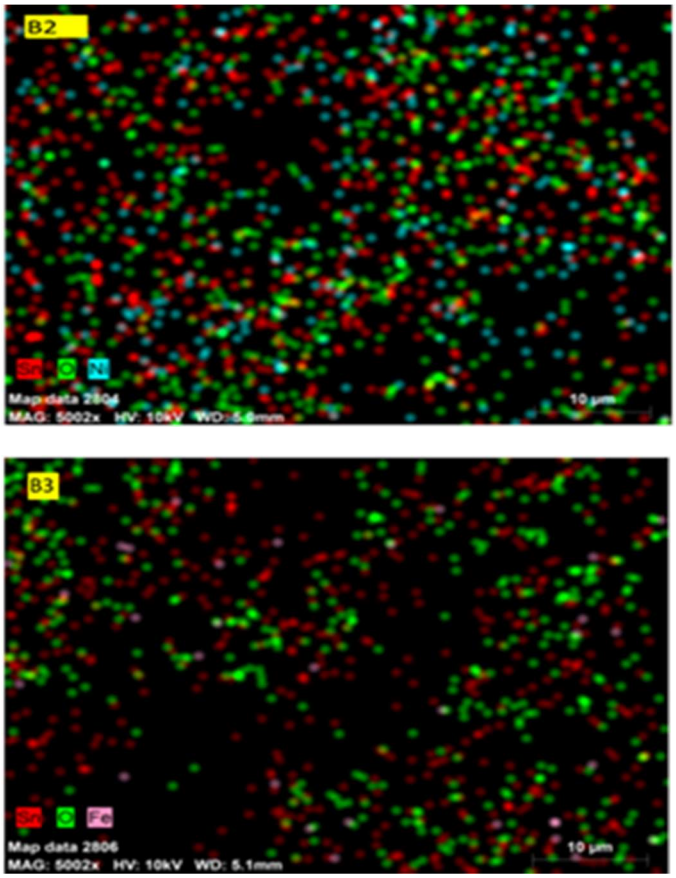

Fig. 4. EDS report of Mapped data (B2) Ni doped SnO_2 and (B3) Fe doped SnO_2 Nanoparticles.

After the doping with Ni and Fe there morphology changes to show porous rock-like structure and which is effectively shown in figure 4. As per EDS analysis the Ni and Fe element having 15.48 wt % and 0.20 wt% respectively was doped in SnO_2 separately shown in Table 2, the surface morphology indicate that the Ni-doped material was become more porous material shown in figure 2 (A2) and Fe-doped material generates the holes shown in figure 2 (A3). However, the holes and porous material is helping to enhance the conductometric behaviour of synthesised material. Elemental mapping technique has been used for the visual identification of the spatial distribution of elements in the material shown with colours Figure 4 (B2) show the Ni-doped SnO_2 and Figure 4 (B3) show the Fe-doped SnO_2 EDS mapping analysis. This mapping images of EDS confirm the doping of the Ni and Fe elements in SnO_2.

Table 2. EDS analysis of atom and weight percentage of elements.

Compound	Undoped SnO_2		Ni-doped SnO_2		Fe-doped SnO_2	
Elements	Atomic %	Weight %	Atomic %	Weight %	Atomic %	Weight %
Sn	29.49%	75.63%	19.07	56.45	22.01	67.59
O	70.51%	24.37%	70.35	28.07	77.85	32.21
Ni / Fe	-	-	10.58	15.48	0.14	0.20
Total	100.00	100.00	100.00	100.00	100.00	100.00

Gas sensing Properties:

Optimum operating temperature

The optimum operating temerature is the most effective term for checking gas sensing of toxic and volatile gases. The temperature and relative humadity both the terms are interconnected with each other in relation to gas sensing and responsible for the physiosorption and chemisorption reaction on the nanomaterial surface. When the temperature of the environment is increses then the water molecule holding capacity of the air is increses then relative humadity of the environment is decrese and vice varsa. Hence, these tems are directly proportinal to each other. The graphic depicts the best gas reaction during a cooling cycle at temperatures ranging from 200 to 40°C. The change in output voltage can be used to determine the increased resistance of the film sensor. When exposed to a specific oxidising or reducing gas, the resistance of the film sensor remains constant, and this resistance may be precisely determined using Ohm's law. In the Figure 5 gas sensor Ni doped SnO_2 and Fe doped SnO_2 give response to the H_2S, C_2H_5OH, NO_2 and NH_3 gases at 80°C and 160°C respectively. At this constant temerature these gases show the different sensitivity percentage. Herein, Ni-doped SnO_2 shows the H_2S (78.20%), C_2H_5OH (42.20%), NO_2 (21.20%) and NH_3 (11.30%) where as for Fe-doped SnO_2 shows the H_2S (6.20%), C_2H_5OH (8.20%), NO_2 (72.20%)and NH_3 (34.20%) sensitivity. As shown in Fig 2 the Ni-doped SnO_2 sensor gives excellent responses to H_2S, with low responses to Ethanol, Nitric Oxide and Ammonia. Thus Ni, doped SnO_2 has excellent selectivity towards the H_2S gas as well as Fe-doped SnO2 sensors shows maximum response toward the NO_2 gas.

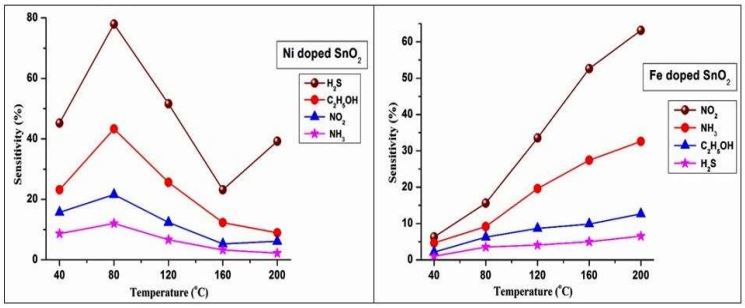

Fig. 5. Gas sensitivity of the Ni and Fe doped SnO_2 sensors of optimised operating temperature.

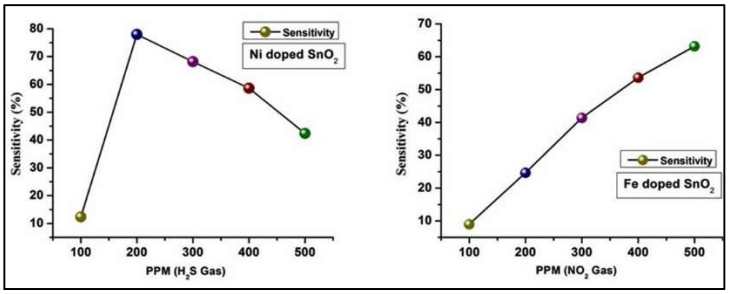

Fig. 6. Gas concentration in ppm variation for Ni-doped SnO_2 and Fe doped SnO_2

The gas concentration ranging from 100 to 500 ppm was utilized to assess the sensory capabilities of the generated doped nanoparticles. Where the Ni-doped SnO_2 check for H_2S gas to obtained 80% sensitivity and Fe doped SnO_2 for NO_2 gas to obtained 40% sensitivity shown in Figure 6. Here the sensing qualities of a semiconductor compound are based on the principle that when the compound is exposed to reducing or oxidizing gases, its conductivity or resistance changes. When reducing gases are used on an object, it makes it more conductive, while oxidizing gases make it more resistant [34].

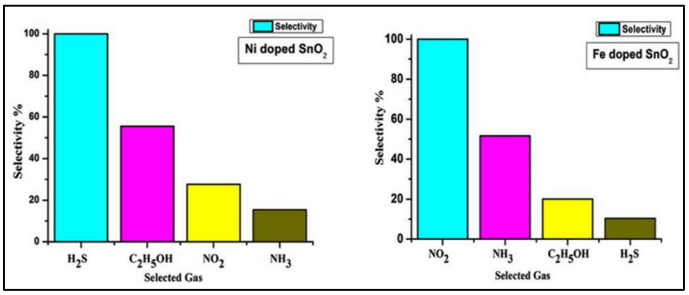

Fig. 7. Gas selectivity ppm variation for Ni-doped SnO_2 and Fe-doped SnO_2 Sensors.

The gas selectivity is a prime aspect of a gas sensor to perform for a particular gas at the desired temperature. Here, the maximum response in Ni-doped SnO_2 gas sensors and Fe doped Gas sensors have been given by H_2S gas vapors and NO_2 gas vapors, respectively. The gas selectivity curves are represented in fig 4. The selectivity of other gases was calculated in ratio with the H_2S gas vapors for the Ni doped SnO_2 and the selectivity of the other gases was calculated in the ratio with NO_2 gas vapors for the Fe doped SnO_2.

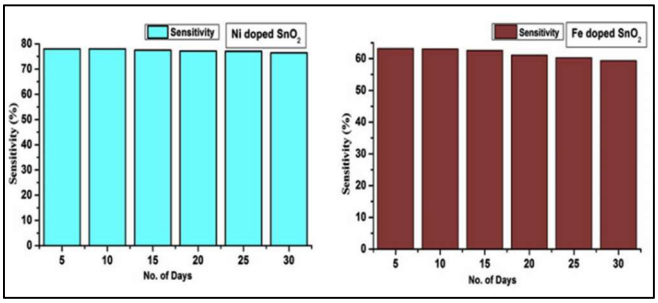

Fig. 8. Reusability graph of synthesized materials.

Another crucial element that governs the real-world uses of gas sensors is stability. As shown in Fig.5 the response value of Ni-doped SnO_2 and Fe-doped SnO_2 sensor to 200 ppm H_2S was not changed much during the 10 days, and after 15 days, the Ni-doped sensor also showed excellent long-term stability, as shown in the graph indicating Ni-doped SnO_2 sensor has excellent short-term and long-term stability and repeatability. The values of reusability shown in Table 3.

Table 3. Reusability test of doped SnO_2

Run	Days of interval	Ni-doped SnO_2 % Response of H_2S	Fe-doped SnO_2 % Response of NO_2
I	5	77	62.30
II	10	77	62.30
III	15	75	61.50
IV	20	75	60.20
V	25	74	60.20
VI	30	74	59.60

Response, recovery study for Ni-doped SnO_2 and Fe-doped SnO_2

There have been four types of methods investigated for the calculation of response and recovery time, such as the flow-through method, the membrane method, the lid method and the gate valve method [35-38]. Figure 9 shows that response time means recess between the immediate variation from clean air to standard H_2S and NO_2 gas is 22s and 30s for the Ni-doped SnO_2 and Fe-doped SnO_2 on the other side, recovery time means recess between the immediate variation from standard H_2S and NO_2 gas to clean air is 44s and 50s for the Ni-doped SnO_2 and Fe-doped SnO_2 respectively. Sensitivity and response have the same meaning in gas sensing.

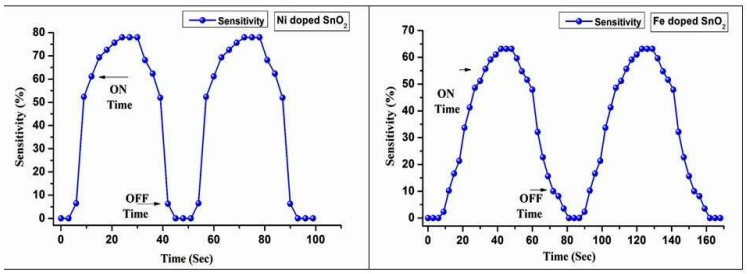

Fig. 9. Transient Sensitivity/Response and recovery time curve of the doped gas sensors.

4. Conclusion

We prepared a Ni-doped SnO_2 sensor and a Fe-doped SnO_2 sensor with ease. Co-precipitation procedure, the gas sensing experiment demonstrated the improved gas sensing efficacy of the Ni-doped SnO_2 sensor and Fe-doped SnO_2 sensor. At 200 ppm H_2S gas vapor, the sensitivity of sensors based on Ni-doped SnO_2 Sensor is up to 80 °C. Such a gas sensor based on Ni-doped SnO_2 could be used reliably for H_2S gas detection. The gas sensitivity of the sensor indicated that it had a response of 78% (response/recovery) (44/50 s), whose response is significantly greater than that of the pure sample. This also provides an alternative material for detecting H_2S gas.

The gas sensing performance of Fe-doped SnO_2 was also studied. The effect of the operating temperature on the gas responses of NO_2, NH_3, H_2S and C_2H_5OH is analyzed. The

maximum sensitivity of the Fe-doped SnO_2 sensor was shown towards NO_2 at 200 and approximately 500 ppm.

Acknowledgements

Department of Chemistry, Satish Pradhan Dnyanasadhana College, Thane, and the Authors are grateful to the Prin. Dr. A.V.Patil, Mahatma Gandhi Vidyamandir's Arts, Science and Commerce College, Surgana for providing library facilities. Authors are gratefully acknowledged to the SAIF SPPU, Pune (M.S) for SEM and EDX results. The authors also thank STIC Cochin, Kerala, for the XRD results. The authors are very thankful to the Department of Chemistry, ASC College, Surgana.

References

[1] M. Ioannis, S. Elisavet, S. Agathangelos, B. Eugenia, Environmental and Health Impacts of Air Pollution: A Review. *Frontiers in Public Health*., 8 (2020) 1-13. DOI: 10.3389/fpubh.2020.00014

[2] G. Sharma, B. Sinha, P. Jangra, H. Hakkim, B.P. Chandra, A. Kumar, V. Sinha, Gridded emissions of CO, NOx, SO_2, CO_2, NH_3, HCl, CH_4, PM2.5, PM10, BC and NMVOC from open municipal waste burning in India. *Environmental Science and Technology*., 53 (2019) 4765–4774. DOI:10.1021/acs.est.8b07076

[3] V. Florentina, R. Milagros, R. Aime, S. John, F. G. Marta, Sampling and analysis techniques for inorganic air pollutants in indoor air, *Applied Spectroscopy Reviews*., 57 (2022) 531-579. DOI https://doi.org/10.1080/05704928.2021.2020807

[4] M. Halder, S. Chatterjee, Microcontroller Based LPG Gas Leakage Alert System. *International Journal of Engineering and Applied Sciences (IJEAS)*. 6 (2019) 29-31.https://www.ijeas.org/download_data/IJEAS0602007.pdf

[5] M.N. Padvi, A.V. Moholkar, S.R. Prasad, N.R. Prasad, A Critical Review on Design and Development of Gas Sensing Materials, *Engineered Science*. 15 (2021) 20-37. DOI: https://dx.doi.org/10.30919/es8d431

[6] Z. Yunusa, M. N. Hamidon, A. Kaiser, Z. Awang, Gas Sensors: A Review. *Sensors & Transducers*., 168 (2014) 61-75. DOI: file:///C:/Users/WIN%207/Downloads/GasSensorsAReview.pdf

[7] N. A. Isaac, I. Pikaar, G. Biskos, Metal oxide semiconducting nanomaterials for air quality gas sensors: operating principles, performance, and synthesis techniques. *Microchimica Acta*., 189 (2022) 1-22. DOI: https://doi.org/10.1007/s00604-022-05254-0

[8] S. Uma, M.K. Shobana, Metal oxide semiconductor gas sensors in clinical diagnosis and environmental monitoring. *Sensors and Actuators A: Physical*., 349 (2023) 114044. https://doi.org/10.1016/j.sna.2022.114044

[9] N. Goel, K. Kunal, A. Kushwaha, M. Kumar, Metal oxide semiconductors for gas sensing. *Engineering Reports*., 5:e12604 (2023) 1-22. DOI: 10.1002/eng2.12604

[10] U.A. Liebrich, Respiratory and Cardiovascular Effects of NO_2 in Epidemiological Studies. *Encyclopedia of Environmental Health*., (2011) 840-844. https://doi.org/10.1016/B978-0-444-52272-6.00065-9

[11] L. Shakerdi, A. Ryan, Drug-induced hyperammonaemia. *J Clin Pathol*., 76 (2023) 501. doi:10.1136/jcp-2022-208644.

[12] N. Kar, D. Gupta, J. Bellare, Ethanol affects fibroblast behavior differentially at low and high doses: A comprehensive, dose-response evaluation. *Toxicology Reports*., 8 (2021) 1054-1066. https://doi.org/10.1016/j.toxrep.2021.05.007

[13] M. Butts, V. L. Sundaram, U. Murughiyan, A. Borthakur, S. Singh, The Influence of Alcohol Consumption on Intestinal Nutrient Absorption: A Comprehensive Review. *Nutrients*., 15 (2023) 1571. https://doi.org/10.3390/nu15071571

[14] C. S. Maldonado, D.S. Kim, B. Purnell, R. Li, G. F. Buchanan, J. Smith, D. R. Thedens, P. Gauger, W. K. Rumbeiha, Acute hydrogen sulfide-induced neurochemical and morphological changes in the brainstem Toxicology. *Toxicology Mechanisms And Methods*., 485 (2023) 153424. https://doi.org/10.1016/j.tox.2023.153424

[15] C. S. Maldonado, A. Weir, W. K. Rumbeiha, A comprehensive review of treatments for hydrogen sulfide poisoning: past, present, and future. *Toxicology Mechanisms And Methods*., 33 (2023) 183-196. https://doi.org/10.1080/15376516.2022.2121192

[16] L.A. Errico, Ab initio FP-LAPW study of the semiconductors SnO and SnO_2. *Physica B Physics of Condensed Matter*., 389 (2007) 140-144. DOI:10.1016/j.physb.2006.07.041

[17] J. Xu, S. Huang, Z. Wang, First principle study on the electronic structure of fluorine-doped SnO_2. *Solid State Commun*., 149 (2009) 527-531. https://doi.org/10.1016/j.ssc.2009.01.010

[18] K.P. Gattu, A.A. Kashale, K. Ghule, NO_2 sensing studies of bio-green synthesized Au-doped SnO_2. *J Mater Sci: Mater Electron*., 28 (2017) 1. DOI:10.1007/s10854-017-7156-3

[19] X. Haixia, Q. Wenxiu, Solvothermal synthesis of SnO_2 nanoparticles for perovskite solar cells application. *Front. Chem*., 12 (2024) 1361275. doi: 10.3389/fchem.2024.1361275.

[20] S. R. Nihal, A. H. Manpreet, S. Kumar, M. Sharma, S.K. Tripathi, J.K. Goswamy., Synthesis and characterization of Ag metal doped SnO_2, WO_3 and WO_3–SnO_2 for propan-2-ol sensing. *Results in Materials*., 9 (2021) 100127. DOI https://doi.org/10.1016/j.rinma.2020.100127

[21] J.G. Kang, J.S. Park, H. J. Lee, Pt-doped SnO_2 thin film based micro gas sensors with high selectivity to toluene and HCHO. *Sensors and Actuators B: Chemical*., 248 (2017) 1011-1016. https://doi.org/10.1016/j.snb.2017.03.010

[22] V. Dhongade, L. Sharma, A. Kahandal, R.C. Aiyer, K. Rajdeo, C. Tagad, Pd doped SnO_2 based room temperature operable resistive sensor for the detection of ethanol vapors Materials Today: Proceedings., 46 (2021) 6437-6444. https://doi.org/10.1016/j.matpr.2020.12.973

[23] C. Liu, Q. Kuang, Z. Xie, L. Zheng, The effect of noble metal (Au, Pd, Pt) nanoparticles on the gas sensing performance of SnO_2-based sensors: a case study on the

{221} high-index faceted SnO_2 octahedra. *Cryst Eng Comm*., 17 (2015) DOI:10.1039/C5CE01162Ks

[24] M. Ippommatsu, H. Sasaki H. Yanagida, Sensing mechanism of SnO_2 gas sensors. *Journal of Materials Science*., 25 (1990) 259-262. https://doi.org/10.1007/BF00544217

[25] A. P. Sharma, P. Dhakal, D. K. Pradhan, M. K. Behera, B. Xiao, M. Bahoura, Fabrication and characterization of SnO_2 nanorods for room temperature gas sensors. *AIP Advances*., 8 (2008) 095219 https://doi.org/10.1063/1.5050991

[26] Y. Kong, Y. Li, X. Cui, L. Su, D. Ma, T. Lai, L. Yao, X. Xiao, Y. Wang, SnO_2 nanostructured materials used as gas sensors for the detection of hazardous and flammable gases: A review *Nano Materials Science*., 4 (2022) 339-350. https://doi.org/10.1016/j.nanoms.2021.05.006

[27] Y. Masuda, Recent advances in SnO_2 nanostructure based gas sensors. *Sensors and Actuators B: Chemical*., 364 (2022) 131876. https://doi.org/10.1016/j.snb.2022.131876

[28] R. Kumar, Mamta, R. Kumari, V.N. Shingh, SnO_2-Based NO_2 Gas Sensor with Outstanding Sensing Performance at Room Temperature., *Micromachines*.,14 (2023) 728. https://doi.org/10.3390/mi14040728

[29] X.F. Li, X.B. Meng, J. Liu, D.S. Geng, Y. Zhang, *Adv. Funct. Mater*., 22 (2012) 1647.

[30] S. Maheswari, M. Karunakaran, K. Kasirajan, P. Boomi, Trarnsition Metal (Ni) Doped SnO_2 Nanoparticles Synthesized by Co-Precipitation Method. *Sensor Letters*., 17 (2019) 919-923 https://doi.org/10.1166/sl.2019.4165

[31] M. Kuppan, S. Kaleemulla, N. M. Rao, N. S. Krishna, M. R. Begam, M. Shobana, Structural and Magnetic Properties of Ni Doped SnO_2. *Advances in Condensed Matter Physics*., 284237 (2014) 1-5. http://dx.doi.org/10.1155/2014/284237

[32] L. Segueni, A. Rahal, B. Benhaoua, N. Allag, A. Benhaoua, M. S. Aida, Iron Doping SnO_2 Thin Films Prepared By Spray With Moving Nozzle: Structural, Morphological, Optical, And Type Conductivities. Digest *Journal of Nanomaterials and Biostructures.*, 14 (2019) 923-935. https://chalcogen.ro/923_SegueniL.pdf

[33] Scherrer P, Nachrichten von der Gesellschaft der Wissenschaften zu Gottingen (1918) 98-100.

[34] D. Deivatamil, M. J. Abel, N. P. Dyana, R. Thiruneelakandan, J. J. Prince, A comparative study on pure and cobalt doped manganese ferrite ($Co:MnFe_2O_4$) nanoparticles in their optical, structural, and gas sensing properties. *J Solid State Communications*., 339 (2021) 11450. DOI:10.1016/j.ssc.2021.114500

[35] L. F. Snik, B. Szafraniak, A. Paleczek, D. Grochala A. Rydosz, A Review of Gas Measurement Set-Ups. *Sensors*. 22 (2022) 2557. https://doi.org/10.3390/s22072557

[36] A. Naquash, M. Nizami, M. A. Qyyum, R. S. Al-Hajri, M. Lee, Membrane-assisted natural gas liquids recovery: Process systems engineering aspects, challenges, and prospects. *Chemosphere*. 308 (2022) 136357. https://doi.org/10.1016/j.chemosphere.2022.136357

[37] Z. Lin, X. Sun, T. Yu, Y. Zhang,; Y. Li, Z. Zhu, Gas–solid two-phase flow and erosion calculation of gate valve based on the CFD-DEM model. *Powder Technology*. (2020) 366. DOI:10.1016/j.powtec.2020.02.050

[38] L. B. Brett, G. Black, P. Moretto, J. Bousek, A comparison of test methods for the measurement of hydrogen sensor response and recovery times. *International journal of hydrogen energy*. 35 (2010) 7652-7663. doi:10.1016/j.ijhydene.2010.04.139